JOURNAL OF MATERIALS SCIENCE 22 (1987) 1808–1814

A study in the work-hardening behaviour of austenitic manganese steels

S. B. SANT, R. W. SMITH
Department of Metallurgical Engineering, Queen's University, Kingston, Ontario, Canada

The work-hardening behaviour of Hadfield's steel and the effect of vanadium additions have been examined. At room temperature, deformation twinning plays a significant role. The rate of work-hardening was found to be sensitive to the presence of vanadium above 1 wt%. Transmission electron microscopy studies indicate that the work-hardening is due to a combination of structural defects. The mechanical behaviour of the alloys in compression can be described by a mathematical expression derived from the familiar Ludwik expression.

1. Introduction

In 1882, Sir Robert Hadfield patented a steel containing 1.2 wt% carbon and 12.5 wt% manganese and possessing such exceptional toughness and impact wear resistance that a century later, the basic alloy, occasionally with minor additions, is referred to as Hadfield's steel and continues to find extensive use in railroad track components and rock crushing equipment [1].

Following casting, Hadfield's steel is usually homogenized above 1323 K (1050° C) to dissolve carbides and then water-quenched to provide a uniform austenitic structure. It is used mainly in this condition. In the absence of an inert atmosphere, the high solutionizing temperature normally produced considerable surface decarburization and the loss of manganese leading to the formation of surface α-martensite upon quenching [2]. The tensile strength and ductility are somewhat affected by composition and heat treatment [1].

The most remarkable property of Hadfield's manganese steel and the one industrially exploited is its exceptionally large work-hardening capacity. There have been a number of investigations to identify the mechanism(s) leading to this behaviour, but the situation is rather unclear. The present study was undertaken in an attempt to resolve the reported ambiguities in room temperature work-hardening behaviour as has been done for austenitic stainless steel [3]. In this study an attempt has also been made to correlate the flow stress–strain curves with microstructural features.

2. Experimental procedure

Compression and impact test specimens of Hadfield's Steel and alloys with "modified" chemical compositions were produced by investment casting using sections of regular rails as melting stock to which alloying additions were made. Table I gives the composition (wt%) of the different alloys studied. They were austenitized at 1423 K (1150° C) for 2 h in an inert atmosphere of argon, then water-quenched. This produced a completely austenitic structure in all the various alloy compositions. The argon atmosphere prevented decarburization. Due to the pronounced difficulty in machining Hadfield's steel, the quenched samples were surface-ground to obtain the desired dimensions for the impact and compression tests. The impact specimens were standard ASTM Charpy specimens, and were tested on a Tinius Olsen impact tester. The compression specimens were in the shape of rectangular blocks 20 mm long with a 100 mm^2 cross-section. All compression tests were performed on an Instron TTD-L unit using a 89 kN (20 000 lbs) GR load cell. The cross-head speed was kept constant at 8.47×10^{-6} m sec^{-1} (0.02 inch min^{-1}) giving an initial strain rate of 4.23×10^{-4} sec^{-1}. The test pieces were placed between two anvils whose faces were protected by hardened steel face plates. The bottom anvil had a ball and socket arrangement with a flat machined into the ball. This allowed for rotational freedom to further ensure a uniaxial stress state during deformation. To minimize barrelling, the ends of the specimen were lubricated. This treatment was sufficient to confine any measureable barrelling to the last 1% or so of the compression range used.

Specimens for transmission electron microscopy were prepared by trepanning rods of 3 mm diameter from transverse sections of the compressed samples

TABLE I Compositions and mechanical properties of austenitic manganese steels

Alloy	% C	% Mn	% V	Yield strength (MPa)	Impact energy (Nm)
R3	1.2	13.0	–	304.8	148
R16	1.2	13.0	1.0	292.5	40.7
R4	1.2	13.0	2.0	366.5	19
R6	0.8	13.0	–	267	154.5
R9	0.8	13.0	1.0	303.2	81.3
R7	0.8	13.0	2.0	318	34

0022–2461/87 $03.00 + .12

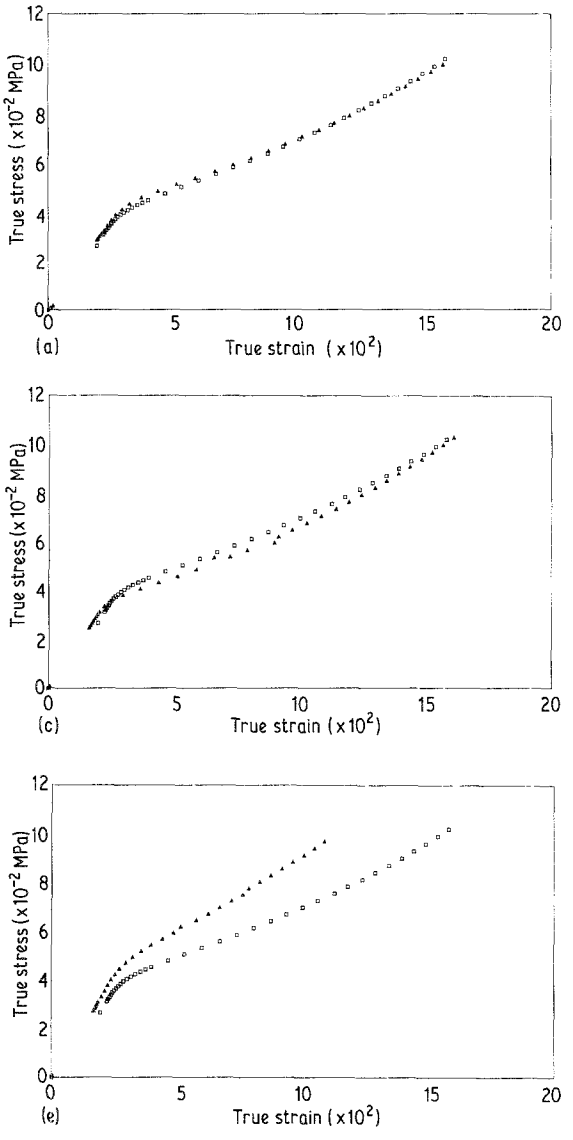

Figure 1 True stress–strain curves of room temperature compression tests. (a) Alloys (□) R3 and (▲) R16, (b) Alloys (□) R3 and (▲) R4, (c) Alloys (□) R3 and (▲) R6, (d) Alloys (□) R3 and (▲) R9 and (e) Alloys (□) R3 and (▲) R7.

using an electro-discharge machine (EDM). From this rod, thin discs of thickness 0.2 mm were sliced. These discs were ground to a thickness of about 0.1 mm on 600 grit paper and were then electro-thinned usng a "TENUPOL 2" unit at a current of 30 mA and a voltage of 40 V d.c. for 3 to 5 min in an electrolyte of 80 g of sodium chromate dissolved in 420 ml of glacial acetic acid at room temperature. In all cases fresh electrolyte was used to prevent the formation of surface artifacts. These thin foils were studied using a Phillips EM400T Scanning Transmission Electron Microscope.

3. Results and discussion

3.1. Flow stress–strain curve

Fig. 1 shows true stress–strain curves for the alloys studied with the yield stress values collected together in Table I. It is seen that all the alloys studied, shown in Fig. 1, show an initial linear (elastic) region followed by the work-hardened stage. Fig. 2a shows part of the original load-compression graph for the standard Hadfield's steel (alloy R3). This graph shows the jerky flow which was also observed for all the other alloys.

In an attempt to quantify the mechanical response of the alloys, a mathematical expression for the plastic region of the true stress–strain curves was developed. In this, the flow curve is plotted on logarithmic coordinates to fit the familiar Ludwik expression [4], namely:

$$\sigma = K\varepsilon^n \quad (1)$$

as shown in Fig. 2b.

It was found that the above expression was obeyed closely over the strain range 0.03 to 0.08. At smaller and larger strains there was a negative and a positive deviation, Δ_1 and Δ_2, respectively (Fig. 2b). It was also found that the logarithms of the deviations bear a linear relationship to the true strain at which they occur, as shown in Fig. 3. Thus,

$$\Delta_1 = \exp(n_1\varepsilon + k_1) \quad (2)$$

and

$$\Delta_2 = \exp(n_2\varepsilon + k_2) \quad (3)$$

These may be incorporated into Equation 1 to produce the following general expression for the flow curves of Hadfield's Steel and its alloys

$$\sigma = K\varepsilon^n - \exp(n_1\varepsilon + k_1) + \exp(n_2\varepsilon + k_2) \quad (4)$$

where σ is the true stress, ε is the true strain, and K, n, k_1, k_2, n_1, n_2, are constants for a given alloy and are shown in Table II.

TABLE II Flow stress–strain equation constants

	K	n	k_1	n_1	k_2	n_2
R3	1775	0.42	8.80	−360.8	−0.25	7.2
R16	1547	0.36	1.60	−46.5	−0.40	8.46
R4	2062	0.48	2.14	−70.1	−0.62	11.8
R6	2100	0.40	2.07	−64.4	−0.45	10.3
R9	1124	0.37	2.16	−86.0	−0.19	7.35
R7	2623	0.49	1.67	−59.4	−0.21	8.23

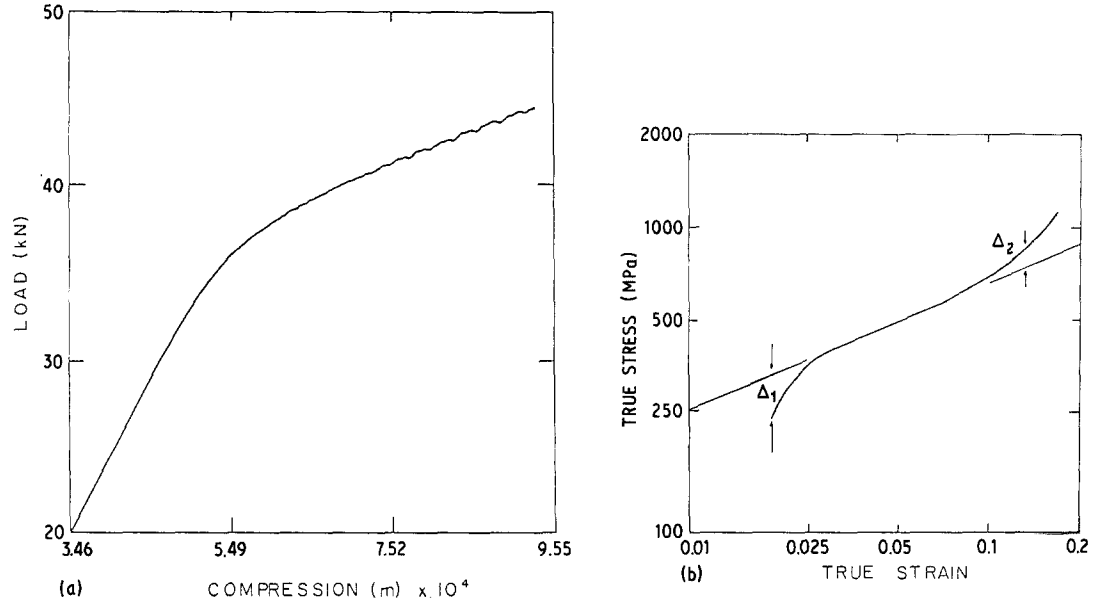

Figure 2 (a) A section of the original load-compression graph of alloy R3, showing the jerky flow. (b) True stress–strain curve of alloy R3 plotted on logarithmic co-ordinates. Deviations Δ_1 and Δ_2 are shown.

The reduction of the stress–strain curve, and thus the work-hardening behaviour of a material to an algorithm is a frequently-used approach to effect a quantitative comparison of the mechanical behaviour of different alloys. During the deformation process, the steel reacts to the imposed forming strains by developing progressively greater internal stresses as a result of the increased difficulty of dislocation motion. This stress reaction to the imposed strain characterizes the plastic behaviour of the steel and is described quantitatively, for a given mode of strain, by the flow curve.

The stress–strain curve obtained for each of the various alloys show similar behaviour and can be generally interpreted in terms of dislocation motion. For convenience, the mechanical behaviour can be considered to consist of three parts, namely behaviour at, (i) small strains, (ii) intermediate strains and (iii) large strains, i.e. where the mechanical response of the material falls below, parallels, and rises above, respectively, the plot according to the Ludwik relationship, Fig. 2b.

(i) At plastic strains below 0.03, the negative deviation can be visualized in terms of dislocations which can move very freely since there are too few defects to pin them effectively and so prevent their motion. (ii) In the intermediate plastic strain range, $0.03 < \varepsilon < 0.08$ the Ludwik expression is obeyed. In terms of dislocation motion this may be interpreted as a proportional increase in obstacles to glide as a result of the formation of defects such as twins and stacking faults with increase in strain. Thus when the applied stress has

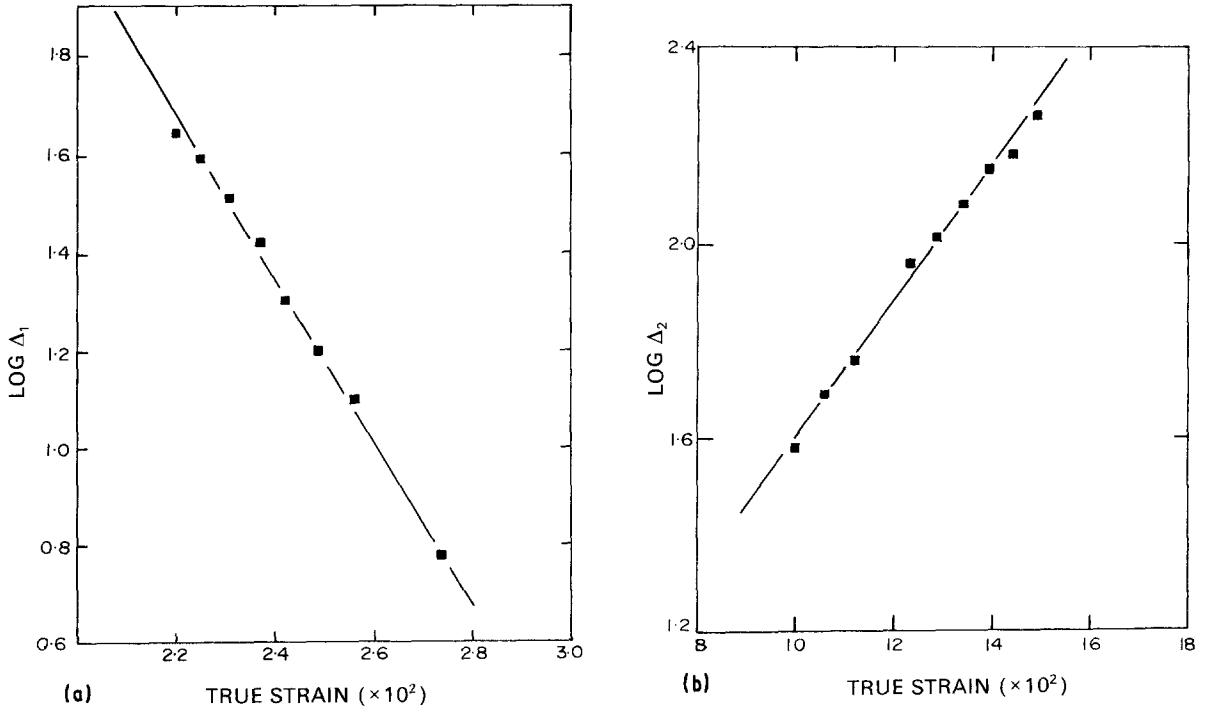

Figure 3 (a) A graph of Log Δ_1 against true strain. (b) A graph of Log Δ_2 against true strain.

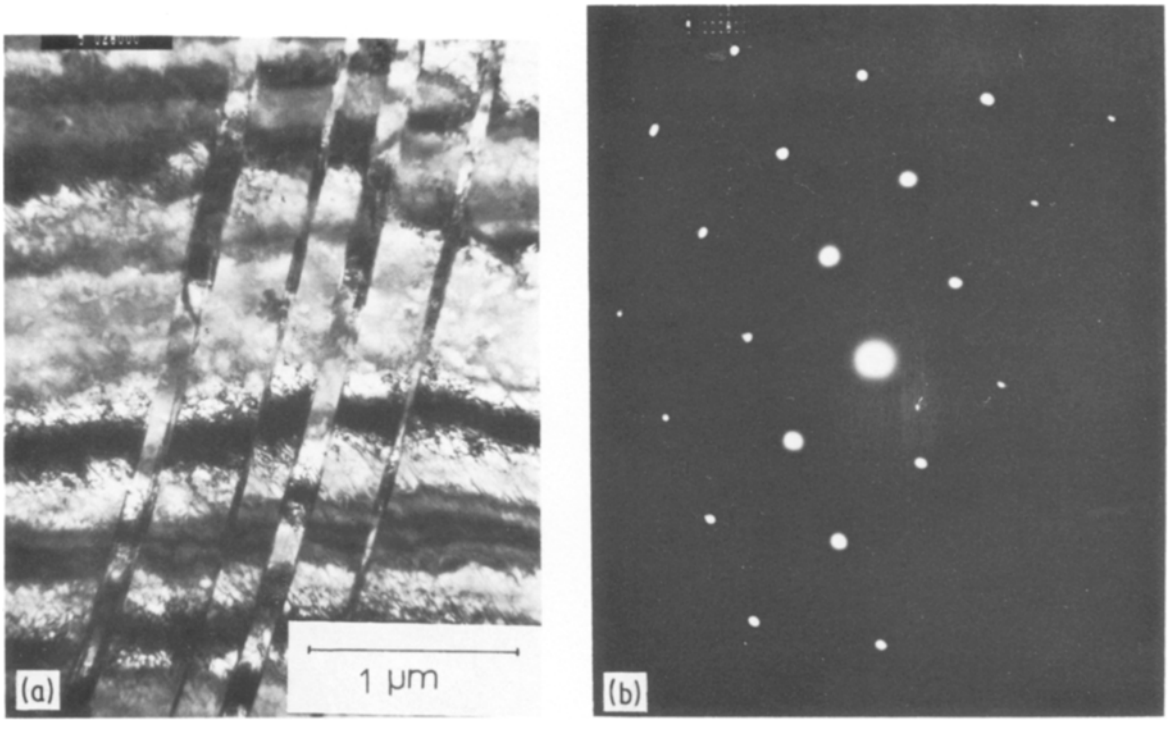

Figure 4 Transmission electron microscopy on deformed standard Hadfield's steel (R3). (a) Deformation twins, (b) Selected area diffraction from the austenite matrix only, (c) Selected area diffraction from deformation twin and austenite matrix. The extra twin spots can be seen. (d) Diffraction pattern shown in (c) after indexing. (○) f c c austenite spots, (×) f c c twin spots. (e) and (f) bright field and dark field electron micrographs showing twins.

exceeded some lower value, mobile defects are generated. However, it is likely that there is constant pinning of the dislocations as well as the generation of new ones; i.e. a situation arises wherein there is pinning and movement of dislocations. This competition gives the linear range and as more dislocations are pinned, proportionately higher stresses are required to generate new ones and keep them in motion. (iii) Above plastic strains of approximately 0.08, for all the alloys tested, there is a positive deviation from the Ludwik expression on a logarithmic scale. At these high strain levels, it is presumed that the defects produced interact more closely and provide an accelerating rate of work-hardening.

3.2. Effect of vanadium on the mechanical properties of Hadfield's steel

The mechanical properties considered here are the yield stress, work-hardening rate and toughness (impact energy absorbed). The values obtained for particular alloys are shown in Tables I and II. However a detailed comparison of the stress–strain curves of the various other alloys with that of the standard Hadfield's alloy (R3), provides considerable insight towards understanding the influence of vanadium on the mechanical properties of Hadfield's steel. In the standard alloy, a significant contribution to the enormous work-hardening capacity is believed to arise from the presence of a number of twins during deformation [5]. However, the addition of vanadium in excess of 0.4 wt % to the standard alloy results in the precipitation of fine carbides [6]. The presence of these would be expected to produce a reduced toughness. The formation of vanadium carbide precipitates will reduce the amount of carbon remaining in solid solution in the matrix. Thus the work-hardening capacity of the matrix would be expected to fall unless significant contribution arose from (a) the precipitation hardening associated with the presence of vanadium carbides in the matrix and (b) strain-induced martensite formation in a carbon depleted matrix.

The yield stress of the alloy would be expected to increase as the solute content of the matrix and volume fraction of finely dispersed precipitate both increased. Figs 1a to e gives the stress–strain curves for the five new alloys (R4, R6, R7, R9 and R16) with the curve for the standard alloy (R3) present as a bench mark for comparison. Close comparison of the various curves suggest that:

(a) Without vanadium present, a reduction in carbon content produces an alloy with similar work-hardening rate and toughness but a smaller yield (R6 against R3).

(b) For a given carbon content, but with 1% vanadium, the alloys produced have similar work-hardening rate and yield strength but impaired toughness (R3 against R16 and R6 against R9).

(c) For a given carbon content, but with 2% vanadium, the work-hardening rate increases, the yield strength increases, and the toughness falls dramatically (R3 against R4 and R6 against R7).

Further detailed experimental work is in progress to explain the behaviour of these alloys. However, the broad range of the influence of vanadium is clear, namely, (i) additions of about 1% produce little change except a reduced toughness and (ii) additions of about 2% produced markedly greater work-hardening but

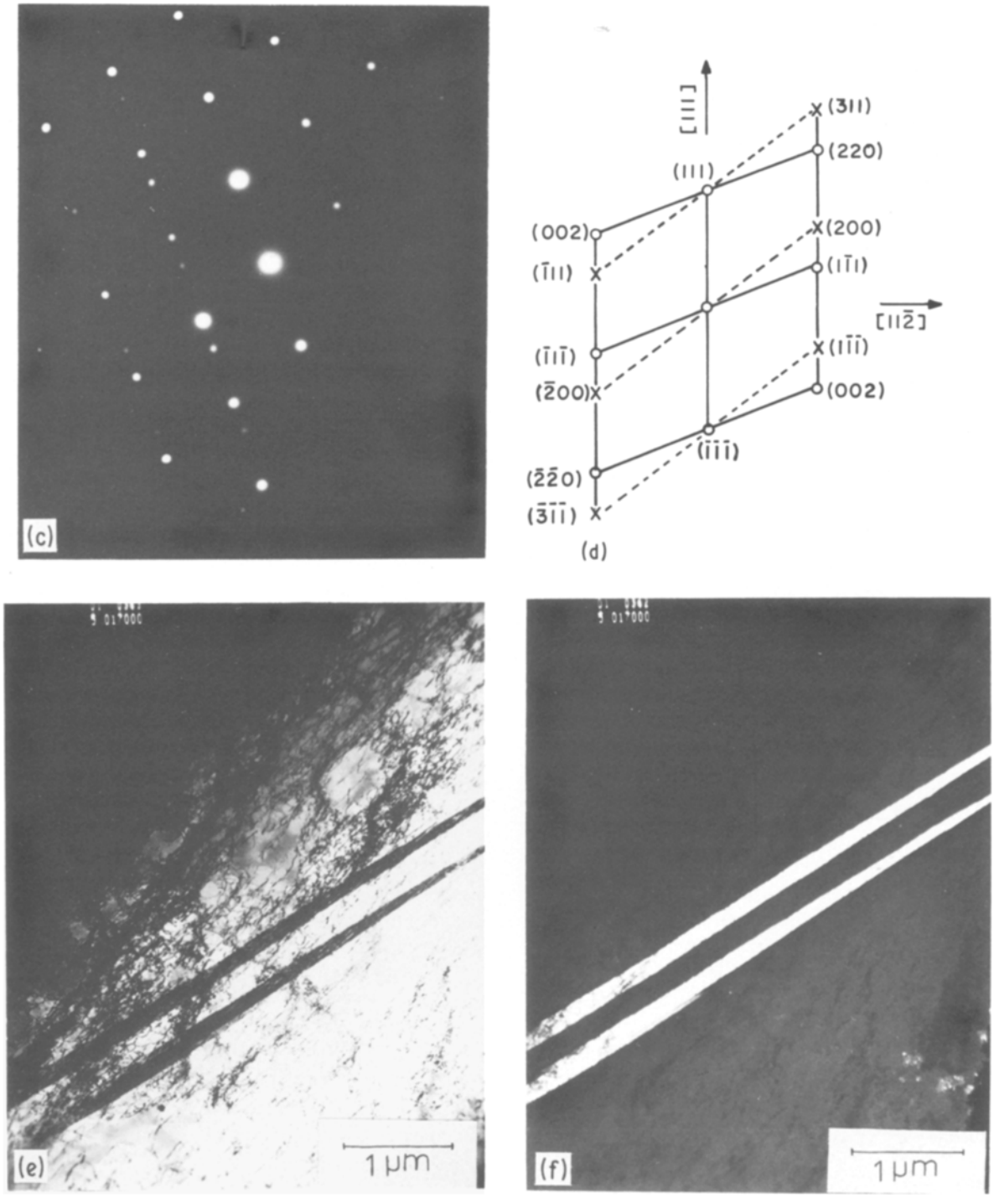

Figure 4 Continued

sharply reduced toughness. A bonus reported elsewhere [6, 7] arising from the presence of vanadium carbides is a much improved wear resistance.

4. Microstructure

4.1. Standard Hadfield's steel

Initially, transmission electron microscopy was carried out on deformed standard Hadfield's steel (R3). Fig. 4 shows electron micrographs and diffraction patterns from R3. These confirm the presence of twinning as was observed under an optical microscope. These deformation twins cut through the austenite matrix which consists of a dense network of dislocations. An electron diffraction pattern taken from the matrix is shown in Fig. 4b. Fig. 4c shows the electron diffraction pattern taken from the twin/matrix interface of Fig. 4a and hence the diffraction spots arise from the lattice planes in both the twin as well as the austenite matrix. The diffraction pattern of Fig. 4c after indexing the spots is shown in Fig. 4d. This conforms to a face-centred-cubic crystal structure showing no evidence of the formation of martensite. Figs 4e and f show bright field and dark field electron micrographs for the standard Hadfield's steel, the latter taken with a twin diffraction spot. The microstructural features observed in this alloy from the present study are very similar to those identified by Roberts [8], Nishiyama *et al.* [9], Raghavan *et al.* [10], Dastur and Leslie [11], and Adler [12] as deformation twins.

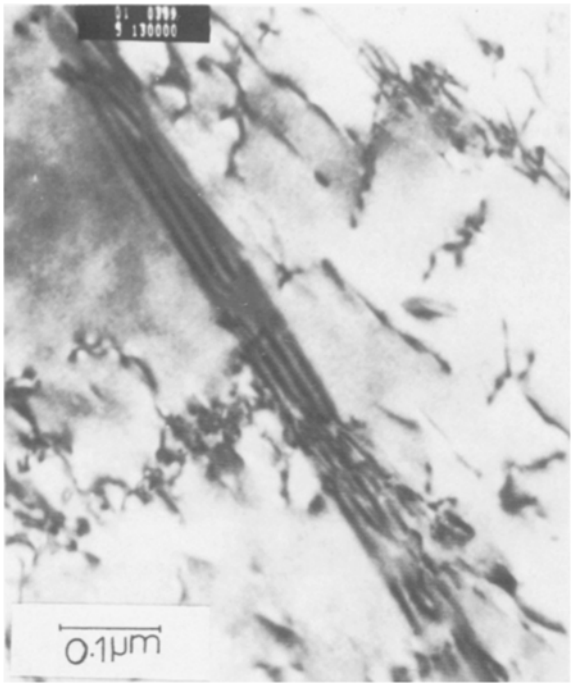

Figure 5 TEM bright field of R16 showing a highly faulted region.

4.2. Effect of vanadium

1% vanadium was added to the standard Hadfield's steel giving alloy R16. Transmission electron microscopy showed the presence of deformation twins as in alloy R3. In addition, at higher magnifications, stacking faults were observed as can be seen in Fig. 5.

Fig. 6 shows an electron micrograph and a diffraction pattern from a deformation sample containing 2% vanadium in Hadfield's steel, alloy R4. Once again it is observed that there is a distinct substructure. The spots on the diffraction pattern arise from the matrix/substructure interface. As a result, although some spots arise from f c c lattice planes; there are others which conform to the h c p crystal structure. In addition to these two crystal structures being present there are a few streaks in the diffraction pattern. As noted above, such streaks indicate the presence of stacking faults and/or thin twins. Thus this alloy consists of f c c (austenite) matrix, and contains ε-martensite which is h c p and a number of stacking faults/thin twins. The zone axis of the f c c diffraction spots is $\langle 0\,\bar{1}\,1 \rangle$ and is one of the zone axes that cannot distinguish between twins and h c p plates in an f c c matrix [13]. Further work is in progress to determine the dominant features giving rise to the increased work-hardening behaviour of this alloy.

Early studies of the work-hardening of this material showed the formation of α- and ε-martensite upon deformation [2]. This has been associated with surface decarburization and loss of manganese during the heat-treatment process.

It has been shown that the addition of alloying elements will lower the stacking fault energy [14]. This leads to an increase in the faulted region. On a microscopic scale the presence of numerous stacking faults appears as a region having an apparent h c p stacking sequence. The theory for f c c → h c p martensite transformation put forward by Olson and Cohen [15, 16] appears to be applicable. Stacking fault formation and twin formation may be considered, from a structural standpoint, as precursors to strain-induced h c p martensite formation.

At room temperature, the standard Hadfield's steel work-hardens mainly due to deformation twinning. The addition of vanadium in excess of 1 wt % leads to the precipitation of carbides even after annealing at 1050° C and water quenching. This leads to a decrease in the amount of free carbon in solution in matrix. This is essentially similar to that produced by decarbu-

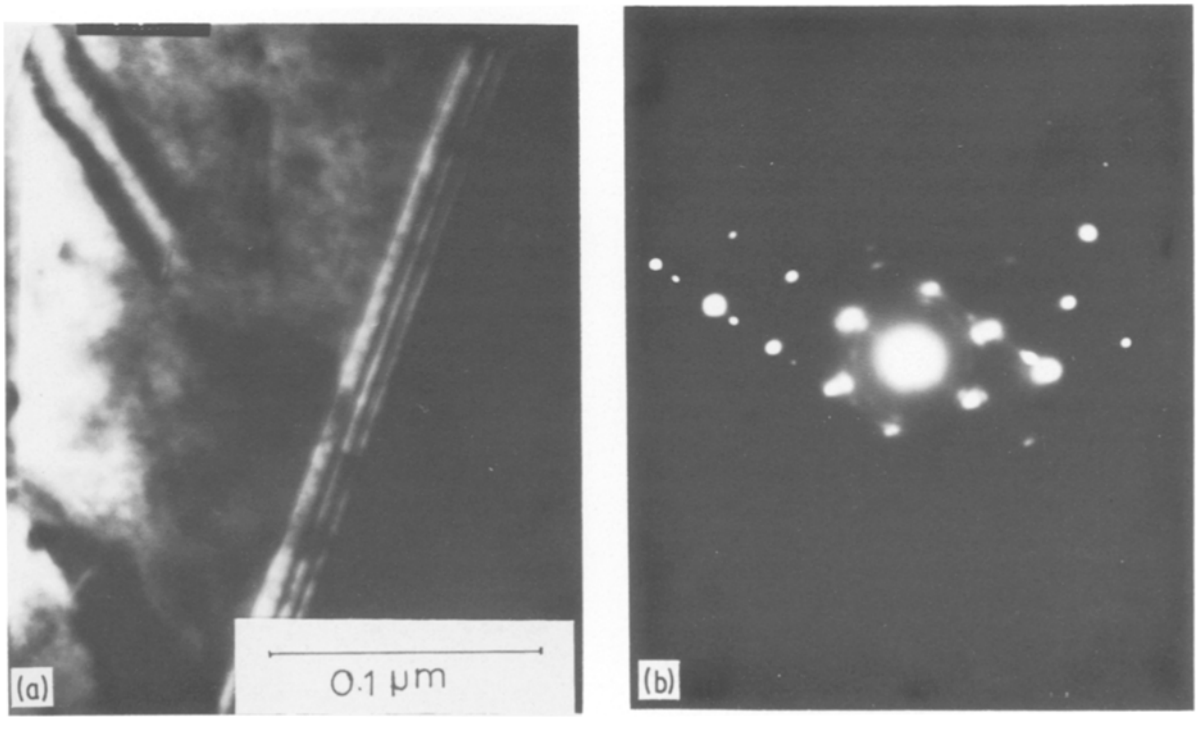

Figure 6 Transmission electron microscopy on deformed alloy R4. (a) Bright field showing twin-faults. (b) Selected area diffraction from the austenite and twin-fault.

rization as observed by White and Honeycombe [2]. As can be seen from the micrographs, the addition of vanadium appears to decrease the amount of deformation twinning while increasing the susceptibility to the formation of hcp martensite. The presence of ε-martensite in alloy R4 could explain the increase in work-hardening compared to alloy R3.

From the microstructural features observed, optically and by electron microscopy, both twins and stacking faults are observed. In addition under appropriate conditions, the formation of epsilon martensite which has a hcp crystal structure could occur. All of these act as obstacles to dislocation motion and results in the high work-hardening capacity.

5. Conclusions

The main conclusions that can be drawn from this study are:

1. Deformation twinning is the primary mechanism for the high work-hardening behaviour in Hadfield's steel at room temperature.

2. Lowering the carbon content of Hadfield's steel from 1.2% C to 0.8% C does not change the work-hardening behaviour appreciably. However the addition of vanadium above 1% does increase the work-hardening characteristics markedly.

3. Mathematical expressions have been generated to describe the flow stress–strain curves of Hadfield's steel and the modified alloys. These generally follow the Ludwik expression at intermediate strains but deviate from it at lower and higher strains. These may be accounted for in terms of dislocation motion during plastic flow. The flow curve can be generally expressed as:

$$\sigma = K\varepsilon^n - \exp(n_1\varepsilon + k_1) + \exp(n_2\varepsilon + k_2)$$

Acknowledgement

The work reported here has been made possible by financial support of the Natural Sciences and Engineering Research Council of Canada, the BILD Programme of the Government of Ontario. This is gratefully acknowledged. The authors would like to thank H. Lagace and ALCAN International, Kingston Laboratories for the use of the STEM, M. Ghoreshy for help in the casting and U. Erb and W. B. F. Mackay for useful discussions.

References

1. HADFIELDS LTD, "Manganese Steel" (Oliver & Boyd, London, 1956) pp. 1–2.
2. C. WHITE and R. W. K. HONEYCOMBE, *J.I.S.I.* **200** (1962) 457.
3. D. C. LUDWIGSON, *Met. Trans.* **2** (1971) 2825.
4. P. LUDWIK, "Elemente der technologischen Mechanik", (Julius Springer, Berlin, 1909).
5. R. E. REED-HILL and J. R. DONOSO, "Review on the Deformation Behaviour of materials", Freund Publishing House Ltd, Tel-Aviv, Israel, Vol. II, 1 (1977) p. 29.
6. A. DeMONTE, PhD thesis, Queen's University, Kingston, Ontario, (1984).
7. V. I. GRIGORKIN, I. V. FRANTSENYUK, I. P. GALKIN, A. A. OSETROV, A. T. CHEMERIS and M. F. CHERNENILOV, *Metallov. i Term Obrab. Met.* **4** (1974) 68.
8. W. N. ROBERTS, *Trans. AIME* **230** (1964) 372.
9. Z. NISHIYAMA, M. OKA and H. NAKAGAWA, *Trans. JIM* **6** (1965) 88.
10. K. S. RAGHAVAN, A. S. SASTRI and M. J. MARCINKOWSKI, *Trans AIME* **254** (1969) 1569.
11. Y. N. DASTUR and W. C. LESLIE, *Met. Trans.* **2** (1981) 749.
12. P. ADLER, MS thesis, M.I.T. Cambridge (1978).
13. H. J. KESTENBACH, *Metallography,* **10** (1977) 189.
14. L. E. MURR, "Interfacial Phenomenon in Metals and Alloys", (Addison Wesley, Reading, Massachusetts, USA, 1975) p. 150.
15. G. B. OLSON and M. COHEN, *Met. Trans.* **7A** (1976) 1897, 1905.
16. M. COHEN and G. B. OLSEN, *J. Less Common Metals* **28** (1972) 107.

Received 7 July
and accepted 9 September 1986